Published in final edited form as:
Pain. 2013 October ; 154(10): 2160–2168. doi:10.1016/j.pain.2013.06.044.

Brain white matter structural properties predict transition to chronic pain

Ali Mansour[1], **Marwan N. Baliki**[1], **Lejian Huang**[1], **Souraya Torbey**[1], **K. Herrmann**[1], **Thomas J. Schnitzer**[2], and **A. Vania Apkarian**[1,*]

[1]Department of Physiology, Northwestern University, Feinberg School of Medicine, Chicago, Illinois, USA

[2]Department of Physical Medicine and Rehabilitation, Northwestern University, Feinberg School of Medicine, Chicago, Illinois, USA

Abstract

Neural mechanisms mediating the transition from acute to chronic pain remain largely unknown. In a longitudinal brain imaging study, we followed patients with a single subacute back pain (SBP) episode for over one year as their pain subsided (SBPr), or persisted (SBPp) representing a transition to chronic pain. We discovered brain white-matter structural abnormalities (in n=24 SBP; SBPp=12 and SBPr=12), as measured by diffusion tensor imaging (DTI), at entry into the study in SBPp in comparison to SBPr. These white matter fractional anisotropy (FA) differences accurately predicted pain persistence over the next year, which was validated in a second cohort (in n=22 SBP; SBPp=11 and SBPr=11), and showed no further alterations over a one-year period. Tractography analysis indicated that abnormal regional FA was linked to differential structural connectivity to medial vs. lateral prefrontal cortex. Local FA was correlated to functional connectivity between medial prefrontal cortex and nucleus accumbens in SBPr. As we have earlier shown that the latter functional connectivity accurately predicts transition to chronic pain, we can conclude that brain structural differences, most likely existing prior to the back pain inciting event and independent of the back pain, predisposes subjects to pain chronification.

Keywords

DTI; prediction; chronic pain; brain; connectivity

1. INTRODUCTION

Chronic pain imparts a large socioeconomic burden (Institute of Medicine of the National Academies report, www.iom.edu, states: chronic pain affects at least 100 million American adults and costs the nation up to $635 billion each year), dramatically degrading quality of life for a large sector of society. Extensive human and animal evidence shows that chronic pain is associated with peripheral and central nervous system reorganization with a large list

*Correspondence should be addressed to: A.V.A. (a-apkarian@northwestern.edu).

Conflict of Interest
The authors report no conflict of interest.

of neuronal and glial changes associated with pain persistence [11]. Moreover, human brain imaging studies indicate that different chronic pain conditions exhibit distinct brain activity and morphological alterations [see reviews [2–4]], and show partial reversal of brain morphology with treatments that reduce the burden of chronic pain [31; 32]. Still, the causal relationship between brain abnormalities and transition to chronic pain remains largely unknown. The critical issue that has remained unresolved is the common clinical observation that, of patients with similar injuries inciting a painful episode, only a minority will proceed to develop chronic pain, which in many cases may persist for a lifetime. The potential respective roles of peripheral afferents and/or central nervous system circuits in pain chronification have been debated for decades [17; 18]. We recently identified the first definitive evidence for a causal biomarker, indicating a causal role of brain functional connectivity in pain chronification [10].

In a longitudinal brain imaging study we followed over a one-year period subjects with a single episode of sub-acute back pain (SBP; no back pain for at least one year prior) as they either recovered (SBPr) or persisted into chronicity (SBPp). We observe that while brain gray matter density decreases and closely reflects the persistent pain of SBPp, corticostriatal functional connectivity (functional connectivity between medial prefrontal cortex, mPFC, and nucleus accumbens, NAc, mPFC-NAc) remains constant over the year, and its strength at a brain scan within weeks after onset of SBP symptoms predicts transition to chronic pain one year later, highly accurately [10]. The functional connectivity was derived from fMRI scans while participants rated the spontaneous fluctuations of their ongoing back pain. Moreover, the number of functional connections between NAc and the cortex were correlated to the affective dimension of back pain in SBPp. Therefore, the mPFC-NAc functional connectivity is a physiological state reflecting the brain's response to back pain, and although it is causally related to pain chronification, it remains unclear whether this is an exaggerated response to the inciting injury, or if the SBPp brain already possesses properties predisposing it to this enhanced functional connectivity. Here we address this issue by examining brain white matter properties within the same longitudinal study. We use diffusion tensor imaging (DTI) scans collected at multiple time points over a one year period, to contrast white matter structural integrity and connectivity between SBPp and SBPr, and to compare to healthy controls and chronic back pain patients (CBP). Our results indicate that white matter properties examined soon after initial pain onset robustly predict pain chronification a year later.

2. Materials and methods

2.1 Subjects

The data presented here are part of an ongoing study in which we examine longitudinal changes in brain structure and function in SBP patients. Participants were recruited throughout the Chicago city area through advertisements in newspapers and the Internet. We recruited 120 SBP patients (duration at presentation of at least 4 but no more than 16weeks), 31 healthy controls, and 31 CBP patients (back pain persisting for > 5 years) into the study.

Brain scans (T1, DTI, fMRI) were conducted on each subject at study entry (baseline, or visit 1, scans done as soon as possible from entry into study; on average at around 12 weeks from onset of back pain; when mean pain was 55.5 ± 2.72 SEM, on a 0–100 visual analog scale, VAS) and we followed their pain and brain markers over four visits for 1 year. All participants were right-handed and were diagnosed by a clinician for back pain. An additional list of criteria was imposed, including pain intensity greater than 40/100 on the visual analog scale and duration of less than 16 weeks. Subjects were excluded if they reported other chronic painful conditions, systemic disease, history of head injury, psychiatric diseases, or more than mild depression (score >19, as defined by Beck's

Depression Inventory). Of the subjects recruited, 34 SBP and 7 healthy subjects dropped out or were removed by visit 2, 22 SBP and 1 healthy subject by visit 3, and 10 SBP patients by visit 4. Some SBP patients who completed the study were removed from the analysis because of missing data. The Institutional Review Board of Northwestern University approved the study.

After checking for aforementioned criteria and image quality at all scans, the pool of remaining subjects included 46 patients with Sub-acute back pain (22 females, 24 males; average age: mean = 42.7 years, SEM = 1.5 years; average education = 14.6 years, SEM= 0.4), 24 patients with chronic back pain (11 females, 13 males; average age: mean = 46.0 years, SEM = 1.6 years; average education = 14.4 years, SEM= 0.4), and 28 healthy controls (12 females, 16 males; average age: mean = 37.7 years, SEM = 2.3 years; average education = 15.1 years, SEM= 2.3). Further demographics and pain characteristics at visits 1 and 4, and their comparisons are summarized in Table 1.

2.1.1 Discovery and validation groups, and white matter regional hypothesis testing—

The first 24 SBP patients with complete DTI data were grouped separately and used to perform a whole-brain white matter skeleton-based voxel-wise search, to identify regional white matter abnormalities (discovery group). The next 22 SBP patients' DTI scans were used for validation. In the validation group only white matter regions identified in the discovery group were examined. This grouping was done a priori and group memberships were kept strictly segregated. We also refrained from performing whole-brain contrasts in CBP and healthy controls, and instead we only tested the white matter regional hypothesis derived from the discovery group.

2.2 Scan acquisition

For all participants and visits, MPRAGE type T1-anatomical brain images were acquired with a 3T Siemens Trio whole-body scanner with echo-planar imaging capability using the standard radio-frequency head coil with the following parameters: voxel size = 1 × 1 × 1 mm, repetition time = 2,500 ms, echo time = 3.36 ms, flip angle = 9°, in-plane matrix resolution = 256 × 256; 160 slices, field of view = 256 mm. DTI images were acquired on the same day using echo planar imaging (72 × 2-mm-thick axial slices; matrix size, 128 × 128; field of view, 256 × 256 mm2; resulting in a voxel size of 2 × 2 × 2 mm). Images had an isotropic distribution along 60 directions using a b value of 1000 $s \cdot mm^{-2}$. For each set of diffusion-weighted data, eight volumes with no diffusion weighting were acquired at equidistant points throughout the acquisition. The total scan time for the diffusion-weighted imaging protocol was approximately 11 minutes. A subset of the participants also underwent fMRI scans with the following parameters: multi-slice T2*-weighted echo-planar images with repetition time=2.5 s, echo time=30 ms, flip angle = 90°, number of volumes = 244, slice thickness = 3mm, in-plane resolution = 64×64. The 36 slices covered the whole brain from the cerebellum to the vertex.

2.3 Image preprocessing

Analysis was performed using tools from the FMRIB Software Library (FSL) (www.fmrib.ox.ac.uk/fsl) and in-house software. DTI data was manually checked volume by volume for obvious artifacts. Afterwards, by utilizing FMRIB's Diffusion Toolbox (FDT), eddy current and simple head motion correction was performed using affine registration to a reference volume (the first no-diffusion weighted volume of each subject). Eddy currents in the gradient coils may cause stretches and shears in the diffusion weighted images, hence the correction. Data, was then skull extracted [33] and a diffusion tensor model was fit at each voxel determining voxel wise fractional anisotropy (FA) [1], which reflects the degree of diffusion anisotropy within a voxel (range 0–1, where large values indicate directional

dependence of Brownian motion due to white matter tracts and smaller values indicate more isotropic diffusion and less coherence) [12].

2.4 Analysis

Voxel-wise statistical analysis of FA data was carried out using the tract-based spatial statistics (TBSS) part of FSL [34]. All SBP subjects' FA data were nonlinearly realigned into a high-resolution common space (MNI standard 1 mm brain). The mean FA image was then created and thinned to create a mean FA skeleton representing the centers of all tracts common to the group. Each subject's aligned FA data was then projected back onto this skeleton. The significance of the contrast between patients and healthy controls was determined using permutation methods (also known as randomization methods) used for inference on statistical maps when the null distribution is not known (n = 5000 permutations, $p < 0.05$, corrected for multiple comparisons). An unpaired t-test model was used, with age as a covariate of no interest. For the area where patients showed a significant difference from control, we extracted individual average FA and compared them between the different groups.

Group maps of the primary diffusion directions (λ_1: axial diffusivity, ($\lambda_2 + \lambda_3$)/2: radial diffusivity to the principal diffusion direction) were calculated. For the area where patients showed a significant FA difference, we tested whether the groups differed in the component diffusivities.

2.4.1 Defining Seeds of Interest for tractography—Easythresh (part of the FSL toolbox) was used to cluster the TBSS resultant significance map into clusters that are ≥50 voxels at p-corrected < 0.05 and p-cluster <0.05. The peak significance voxels from the resultant clusters were then used to manually draw 30 voxel seeds of interest lying within the mean FA skeleton and centered on the peak significant voxel. Each seed was then back projected onto the mean FA skeleton in standard space (i.e., after the FA image had been nonlinearly registered to the target image). Then, this was inverse warped back into the subject's native space, by inverting the nonlinear registration that was originally applied. For each seed, the result was 46 subject space seeds that constitute the tractography seed masks (http://www.fmrib.ox.ac.uk/fsl/tbss/index.html).

2.4.2 Estimation of grey-to-white matter interface and defining targets of interest—FAST (FMRIB Automated Segmentation Tool) was used to segment the 3D T1 image of the brain into different tissue types (Grey Matter, White Matter and cerebrospinal fluid) while also correcting for spatial intensity variations. Compared to most finite mixture model-based methods, FAST is robust and reliable. The underlying method is based on a hidden Markov random field model and an associated expectation-maximization algorithm yielding probabilistic and/or partial maps. For each of the 46 SBP subjects we transformed the grey matter and white matter masks into standard space using FSL linear registration tool (FLIRT). Those masks were then thresholded at (probability > 0.25) and multiplied with each other yielding a subject specific grey-white matter interface composed of regions having relatively equal probabilities of being in either category, thus constituting the grey-white matter boundary (figure 1). The Anatomical Automatic Labeling atlas (AAL atlas) was used to define the medial frontal cortex and the lateral frontal cortex in standard space. Those masks were, then, linearly multiplied by each subject's grey-white matter interface masks to yield 46 subject specific medial and lateral prefrontal cortex grey-white matter target masks (figure 1).

2.4.3 Probabilistic Tractography—We performed probabilistic tractography using FDT software [13] by first running Markov-chain Monte Carlo sampling to build up distributions

on the diffusion parameters at each voxel in the individual subject's space. Afterwards, for each of the seeds of interest, whole-brain probabilistic tractography was run, using PROBTRACKX. 5000 samples were drawn to build the a posteriori distribution of the connectivity distribution. The connection probability between the seed of interest and any one target voxel in the brain is defined as the sum of hits within the target region divided by the sum of hits in the whole ipsilateral hemisphere. The resultant probabilities were then normalized by subject specific target volume (in ml) yielding "normalized connection strengths" between seed and target. Average connectivity maps were generated in MNI space by linearly transforming individual connectivity distributions into MNI 2mm space and then taking the average across each group. For ease of visualization, the mean maps where then thresholded at 100.

2.4.5 Functional connectivity—Thirty-one subjects constituting a sub population of our data set underwent MRI scans while rating magnitude of spontaneous fluctuations of back pain, the details of which are explained in our earlier report [10]. The same seeds of interest (mPFC and NAc) used in the aforementioned report to determine functional connectivity (as determined by temporal coherence of the BOLD signal) were used to extract the mean FA value of the voxels constituting the seeds of interest. The NAc seed was 27 voxels (0.216 ml) and the mpfc seed was 343 voxels (2.7 ml).

3. RESULTS

3.1 Subject demographics

The SBP group was subdivided (20% change in pain intensity from baseline to 1 year) into recovering (SBPr, $n = 23$) and persisting (SBPp, $n = 23$) (Figure 2A). At baseline, SBPp and SBPr had similar durations of back pain (Figure 2B) and showed similar pain and mood characteristics (Table 1); at visit 4 (one year later) SBPr subjects showed decreases in most pain-related measures (Table 1).

3.2 Whole-brain contrast for white matter integrity differences between SBP types

To identify DTI parameters predictive of transition into chronicity, we first arbitrarily divided the SBP subjects into a *Discovery group* (n=24; SBPp=12 and SBPr=12) and a *Validation group* (n=22; SBPp=11 and SBPr=11), and in the discovery group contrasted FA maps between SBPp and SBPr (Figure 2C). Whole-brain voxel-wise comparison over the white matter skeleton, with correction for age as a confound, using permutation testing and stringent statistical thresholding showed that SBPp patients have lower FA values in three clusters: the temporal part of left superior longitudinal fasciculus (slf) (cluster volume = 0.543 ml; with peak decreased FA at coordinates −34, −1, 21; t-value = 4.20, p-corrected = 0.027); a second cluster (0.990 ml) encompassing left retro-lenticular part of the internal capsule (R-Icap: peak coordinates −38, −28, −1; t-value = 4.02, p-corrected = 0.025) and the external capsule (Ecap, peak coordinates −34, −10, −3; t-value = 3.72, p-corrected = 0.031); and a large third cluster (4.62 ml) located in the left anterior limb of the internal capsule (coordinates −15, 10, 5; t value = 5.20, p-corrected = 0.032) and part of the corpus callosum including the anterior corona radiata (peak coordinates −15, −31, 17; t-value = 3.46, p-corrected = 0.022). The opposite contrast, searching for decreased FA in SBPr, was null.

3.3 Regional white matter differences across groups

To generate a single FA value that can be contrasted between conditions and used as a predictive biomarker, we pooled all voxels (z>3.0) from the three clusters to calculate grouped FA (grp-FA) in SBPp and SBPr, and extracted mean FA (from coordinates corresponding to grp-FA) from baseline scans in CBP and healthy controls, and corrected for age confound in each group. A one-way ANOVA comparing grp-FA across SBPp, SBPr,

CBP, and healthy controls was significant ($F_{3, 72} = 23.55$, $p<0.001$) (Figure 2D). Importantly, grp-FA in CBP matched with grp-FA in SBPp (post-hoc comparison shows no statistical difference, $p = 0.9$), and in Healthy controls grp-FA was intermediate to those of SBPp and SBPr and significantly different from both (post-hoc $p =0.006$ and $p < 0.001$, respectively).

3.4 Predicting future SBP groups from white matter integrity

In the discovery cohort, grp-FA at baseline (visit 1) accurately predicted future SBP groupings (using receiver operator curves, ROC, and the area under the ROC curve as discrimination index, D). This prediction was perfectly correct at one year (visit 4 $D = 1.0$, p undefined due to zero mistakes), with significant predictions for shorter durations as well (visits 2 D=0.90, $p<0.05$; visit 3 D=0.81, $p<0.05$) (Figure 2E). To test reproducibility and thus validate this prediction, we extracted the grp-FA values from corresponding coordinates in the validation cohort and examined its properties. In this cohort as well, grp-FA at baseline was significantly lower in SBPp, and significantly accurately predicted SBP groups at one year (D=0.82, $p<0.02$, unbiased estimate) (Figure 2F).

3.5 Diffusivity properties for white matter region differentiating SBP groups

Various combinations of differences in axial and radial diffusion can underlie changes in FA between groups. As both discovery and validation cohort grp-FA differentiated SBP groups and accurately could predict long-term SBP groupings, we pooled grp-FA values from both groups and examined, in 46 SBP subjects, axial, radial, and mean diffusivity for all voxels encompassing grp-FA, as a function of groups, after correcting for age as a confound. Axial diffusivity was significantly larger in SBPr $(12.9 \pm 0.1) \times 10^{-4}$ (in mm^2/sec units) compared with SBPp $(12.4 \pm 0.1) \times 10^{-4}$ ($p<0.01$) (Figure 3A); radial diffusivity was significantly less in SBPr $(4.68 \pm 0.1) \times 10^{-4}$ compared with SBPp $(5.20 \pm 0.1) \times 10^{-4}$ ($p<0.01$) (Figure 3B); whereas mean diffusivity was larger in SBPp $(7.6 \pm 0.1) \times 10^{-4}$ (in mm^2/sec units) compared to SBPr $(7.4 \pm 0.1) \times 10^{-4}$ ($p<0.05$) (Figure 3C). Therefore, water diffusion in the white matter tracts of voxels comprising grp-FA in the SBPp brain is less over the principal fiber direction, and greater over the directions perpendicular to the principal fiber direction yielding an overall increase in mean diffusivity (Figure 3D). Therefore, in SBPp and for the regions comprising grp-FA, we observe a combination of decreased myelination and axonal tract distortion [15; 35], as the flow of water across these white matter tracts are less coherent and more spread along potentially new directions.

3.6 Differential structural connectivity to medial and lateral frontal cortex

To examine the properties of tracts passing through the regions with distinct FA, we used probabilistic tractography and quantified connectivity to medial and lateral frontal cortices, as a function of SBP groupings. Earlier observations [5–7; 23; 32] suggest the general hypothesis that white matter tracts distinguishing between SBP groups may reflect differential structural connectivity to medial and lateral frontal cortices, imparting vulnerability towards, or protection against, pain chronification. Of the clusters showing reduced FA in SBPp, peak coordinates were used to generate seeds of interest, and normalized probabilistic connectivity were calculated for the two targets, based on subject specific gray-white matter boundary (figure 1). The seeds of interest were left Ecap (−34, −10, −3), left r-Icap (−38, −28, −1), left temporal part of slf (−34, −1, 21), left anterior corona radiata (−15, −31, 17) and left anterior limb of Icap (−15, 10, 5). Only three (of 5) seeds showed differential connectivity: Tracts seeded from Ecap showed increased normalized connection strength to the medial frontal cortex in SBPp (0.42 ± 0.04 as compared to SBPr 0.26 ± 0.04). Similarly, from r-Icap we observe preferential medial frontal cortex connectivity in SBPp (0.42 ± 0.05 as compared to SBPr 0.27± 0.04). However, from the temporal slf connectivity was higher to the lateral frontal cortex in SBPr

(1.11± 0.09 as compared to SBPp 0.85± 0.08) (Figure 4B, 4C). When these seed to target connections were examined one year later we only observed a significant further increase in connectivity between slf and lateral prefrontal cortex in SBPr (Table 2).

3.7 Relationship between microstructure and functional connectivity

Given that mPFC-NAc functional connectivity accurately predicts chronification of pain [10] and the regions with abnormal FA that we observe in the current analysis were located in close proximity to the basal ganglia, we hypothesized that the functional connectivity may reflect underlying structural properties. To this end, we extracted FA values for NAc and mPFC (using coordinates derived from [10]) and tested their relationship to each other and to mPFC-NAc functional connectivity (15 SBPp and 16 SBPr for whom both DTI and fMRI data was available at baseline). We observed that, in SBPr, NAc FA was positively correlated to mPFC FA ($R=0.61$, $P<0.05$) and to NAc-mPFC functional connectivity ($R=0.57$, $p<0.05$, $n=16$), neither correlation exists in SBPp ($R=0.19$, $p=0.4$, and $R=0.35$, $p=0.2$ respectively, $n=15$). (Figure 5A, Figure 5B). Moreover, FA in NAc was not different between the two groups ($t_{29} = -1.4$, $p = 0.17$) nor was FA in mPFC ($t_{29} = 0.22$, $p = 0.83$) (Figure 5C). The results demonstrate that microstructural properties of mPFC and NAc are inter-related in SBPr individuals and these properties are also related to the extent of information shared between the two regions. These relationships are absent in SBPp.

3.8 Minimal changes in white matter integrity over a one-year period

To identify white matter FA changes in time for persisting or recovering SBP, we contrasted whole brain voxel-wise FA, between baseline (visit 1) and corresponding FA map one year later (visit 4), separately for SBPp and for SBPr. A paired t-test using permutation testing and stringent statistical thresholding showed no significant differences with time, in either SBPp or SBPr (at lower threshold we observe scattered FA differences that do not survive cluster thresholding). We also examined whether grp-FA values change longitudinally. A two way repeated measure ANOVA showed no time effect ($F_{1, 22} =0.63$, $p=0.44$), but significant effects were observed for group (for SBPp at visit 1 FA $=0.48\pm5.6\times10^{-3}$, and at visit 4 FA $=0.49\pm6.6\times10^{-3}$; mean±SEM; while for SBPr at visit 1 FA $=0.54\pm3.6\times10^{-3}$, and at visit 4 FA $= 0.53\pm6.5\times10^{-3}$) ($F_{1, 22} =36.27$, p □ 0.001) and for group x time interaction ($F_{1, 22} =9.86$, $p=0.005$). Post-hoc comparisons of grp-FA between baseline and one-year were not significant for SBPp, but was slightly (relative to group differences) yet significantly reduced in SBPr ($p <0.01$). In conclusion, FA differences between SBP groupings are observed at baseline and remain essentially invariant over one year.

4. Discussion

Here, we demonstrate an accurate, and validated, prediction of pain chronification based on white matter structural differences. By examining brain white matter properties at a time early after onset of acute back pain, when pain intensity and duration were similar between those whose pain would resolve and those in whom pain would persist, we could predict pain chronification one year later. The general paradigm used – in which longitudinal multi-modal brain imaging data and pain are followed in a cohort with a single event of acute/subacute pain episode that in time diverges into persistent and recovering groups, and where results are contrasted with healthy (negative) controls and with chronic back pain (positive) controls – should be of widespread utility in identifying critical brain parameters involved in pain chronification across various clinical pain conditions. Furthermore, we validated our main finding by dividing the SBP cohort into two, equal sized, subgroups, and demonstrated that in the discovery and validation cohorts local FA differences between groups at baseline accurately predict SBP groups in the future. We found multiple regional FA decreases in the SBPp, in contrast to SBPr, with the overall pattern of FA (across the regions distinguishing

the groups, grp-FA) in SBPp resembling FA in CBP, while the regional FA in SBPr seems to better resemble FA in healthy controls. Although the regional FA (grp-FA) in healthy controls is more similar to SBPr, it is significantly different from both SBPp and SBPr. This may very well be due to the healthy population sharing representatives from both patient conditions (potentially recovering and potentially persisting individuals) which highlights the hypothesis that the propensity to pain chronification is an a priori disposition awaiting an inciting event. Importantly we see very small changes in FA values longitudinally only in SBPr, over a one-year period. Genetic studies comparing monozygotic and dizygotic twin pairs have shown that genetic factors explain 75% to 90% of variance in white matter [36]; this along with the temporal near constancy of FA, as well as the SBP group FA correspondences with healthy and CBP groups altogether suggest that the FA differences between SBP groups are primarily independent of the pain state and thus a predisposition. Although multiple lines of evidence indicate that brain white matter integrity is most likely a predisposition, we still cannot completely rule out the (unlikely) possibility that the burden of back pain may have been significantly higher in SBPp in the time window from its inception to the time when we recruited them into the study, and that this differential burden may have given rise to the observed FA differences between the two groups. We observe that for the regions where FA was low in SBPp, there are associated changes in diffusivity, and demonstrate differential connections for components of the region to medial and lateral frontal cortex.

4.1 Effect size relative to aging

Multiple studies indicate that white matter FA decreases with aging [14; 22; 29; 37]. Reported results are consistent across labs and generally show that FA, especially in frontal cortex white matter, decreases by about 0.1 over a 60-year age range, and whole-brain skeletal FA decreases by about 0.03 over a 30 year age difference [14; 22; 29; 37]. As the mean age of all three subject groups studied here were within a 10 year range and SBP subgroups showed small but significant age differences, throughout this study we used age as a confound of no interest. Still, comparing between SBPp and SBPr, for the grp-FA, we observe FA difference larger than 0.06, implying that prefrontal white matter in SBPp exhibits 30–50 years of additional aging, in comparison to SBPr or to healthy controls.

4.2 Relationship between functional connectivity and regional FA

Given that mPFC-NAc functional connectivity predicts future pain [10], we examined its relationship to corresponding grey matter FA values, to link local FA characteristics with functional properties. Even though mean FA was not different between SBP groups either in mPFC or NAc; only is SBPr NAc and mPFC FA were positively correlated with each other and with NAc-mPFC functional connectivity. SBPp showed an absence of relationship for FA between these regions and with functional connectivity, implying disruption/reorganization of these relationships. However, the precise processes underlying grey matter anisotropy and diffusivity remain unclear, and in the basal ganglia microstructure seems dominated by extent of iron accumulation [20; 30].

4.3 White matter abnormalities across chronic pain conditions

White matter abnormalities, as determined by DTI imaging, have been identified in most neurodegenerative conditions [25; 26; 28; 39]. However, only a handful of studies have examined brain white matter integrity in chronic pain. There is now DTI-based evidence of brain white matter structural abnormalities in complex regional pain syndrome [19], cluster headache [38], irritable bowel syndrome [16], temporomandibular disorder [27] and fibromyalgia [24]. These studies complement present observations, and also suggest that white matter properties are distinct between pain conditions, which is consistent with the accumulating evidence that chronic pain conditions are accompanied with specific brain

functional activity and unique grey matter reorganization [see reviews [2–4]]. Remarkably, when we examine FA in regions derived from the SBP contrast, we observe the same pattern of FA difference between CBP and healthy controls as we observe between SBP groups. This similarity demonstrates that SBPp and CBP share regional FA abnormalities, showing that CBP is accompanied with white matter abnormalities, and also validating our main result with an unbiased observation. More importantly, in light of the current study, brain white matter abnormalities reported in diverse chronic pain conditions should be considered as evidence for structural predisposition for developing these specific chronic pain conditions.

4.4 Differential structural connectivity to medial/lateral prefrontal cortex

Tractography remains too crude a technique to enable dissection of specific pathways that underlie regional FA differences. For this reason we instead examined probabilistic connectivity, from seeds placed at regions distinguishing SBP groups with FA, to all of the medial and lateral frontal cortices. Parts of the medial and lateral frontal cortex compete in acute pain perception [23]; the lateral frontal cortex undergoes gray matter loss in CBP [5], which is reversed with proper treatment [32]; while portions of the medial prefrontal cortex (ACC and mPFC) reflect the back pain of CBP [6; 7] and disrupts the medial prefrontal component of the default mode network [8]. These observations suggest that differential medial/lateral prefrontal structural connectivity may be a component of the process of pain chronification. For the seeds, Ecap and r-lcap, located within or just lateral to the insula, and in close proximity to the basal ganglia, connectivity in SBPp was higher to the medial frontal cortex, and one year later these connections did not change. On the other hand for the seed placed more superiorly in slf, connectivity in SBPr was higher to the lateral frontal cortex, which significantly further increased one year later (and grp-FA also changed in time in this group). As structural connectivity reflects functional connectivity (the opposite relationship is not necessarily true) [21], the tractography results suggest preferential functional information sharing with the medial frontal cortex in SBPp, but not in SBPr, which is consistent with the multiple lines of evidence indicating that mPFC reorganizes in time to reflect the pain of CBP [6–8]. Thus, the preferential information sharing with the medial frontal cortex can be regarded as part of the vulnerability of SBPp to pain chronification. The inverse seems also to be true: in SBPr we observe higher information sharing with lateral frontal cortex, and as these subjects recover from back pain this process is further enhanced suggesting that heightened connectivity to lateral frontal cortex seems both protective as well as part of the mechanisms involved in recovery from SBP.

4.5 Relationship between structural properties and transition to chronic pain

Previous research shows that perception of pain in CBP engages mPFC [7], distorts NAc valuation responses to thermal painful stimuli, and affects the mPFC-NAc connectivity in such a way that when assessed during a painful thermal stimulus this connectivity can differentiate between CBP and controls and reflects the intensity of back pain in CBP [9]. Moreover, this same functional connectivity predicts, at baseline, SBP groupings one year later [10]. In addition here we showed that FA values within mPFC and NAc, at the same coordinates as identified in [10], and their relationship to the strength of mPFC-NAc functional connectivity are also different between SBP groups. Therefore present results, together with those shown in [10], demonstrate that structural properties as measured by FA predispose subjects to pain chronification. The back pain serves as an inciting event and, given a subject's structural propensity, establishes specific functional connectivity strength. If this mPFC-NAc functional connectivity strength is high, then the limbic brain learning circuitry subsequently and continuously reorganizes the grey matter profile of the cortex, which tracts and reflects the properties of the chronic pain state. Furthermore, the present results imply that brain white matter properties are indicators for predisposition to chronic

back pain, pointing to the need for more extensive studies regarding white matter integrity in chronic pain and in chronification of pain.

Acknowledgments

We thank all patients and healthy volunteers that participated in the study. This study was funded by NIH NINDS NS035115 (A.V.A.), M.N.B. was funded by an anonymous foundation.

References

1. Alexander AL, Lee JE, Lazar M, Field AS. Diffusion tensor imaging of the brain. Neurotherapeutics. 2007; 4(3):316–329. [PubMed: 17599699]
2. Apkarian AV, Baliki MN, Geha PY. Towards a theory of chronic pain. ProgNeurobiol. 2009; 87(2): 81–97.
3. Apkarian AV, Bushnell MC, Treede RD, Zubieta JK. Human brain mechanisms of pain perception and regulation in health and disease. Eur J Pain. 2005; 9(4):463–484. [PubMed: 15979027]
4. Apkarian AV, Hashmi JA, Baliki MN. Pain and the brain: Specificity and plasticity of the brain in clinical chronic pain. Pain. 2011; 152(3):s49–s64. [PubMed: 21146929]
5. Apkarian AV, Sosa Y, Sonty S, Levy RE, Harden RN, Parrish TB, Gitelman DR. Chronic back pain is associated with decreased prefrontal and thalamic gray matter density. J Neurosci. 2004; 24:10410–10415. [PubMed: 15548656]
6. Baliki MN, Baria AT, Apkarian AV. The cortical rhythms of chronic back pain. The Journal of neuroscience: the official journal of the Society for Neuroscience. 2011; 31(39):13981–13990. [PubMed: 21957259]
7. Baliki MN, Chialvo DR, Geha PY, Levy RM, Harden RN, Parrish TB, Apkarian AV. Chronic pain and the emotional brain: specific brain activity associated with spontaneous fluctuations of intensity of chronic back pain. J Neurosci. 2006; 26(47):12165–12173. [PubMed: 17122041]
8. Baliki MN, Geha PY, Apkarian AV, Chialvo DR. Beyond feeling: chronic pain hurts the brain, disrupting the default-mode network dynamics. J Neurosci. 2008; 28(6):1398–1403. [PubMed: 18256259]
9. Baliki MN, Geha PY, Fields HL, Apkarian AV. Predicting value of pain and analgesia: nucleus accumbens response to noxious stimuli changes in the presence of chronic pain. Neuron. 2010; 66(1):149–160. [PubMed: 20399736]
10. Baliki MN, Petre B, Torbey S, Herrmann KM, Huang L, Schnitzer TJ, Fields HL, Apkarian AV. Corticostriatal functional connectivity predicts transition to chronic back pain. Nature neuroscience. 2012; 15(8):1117–1119.
11. Basbaum AI, Bautista DM, Scherrer G, Julius D. Cellular and molecular mechanisms of pain. Cell. 2009; 139(2):267–284. [PubMed: 19837031]
12. Beaulieu C. The basis of anisotropic water diffusion in the nervous system - a technical review. NMR Biomed. 2002; 15(7–8):435–455. [PubMed: 12489094]
13. Behrens TE, Woolrich MW, Jenkinson M, Johansen-Berg H, Nunes RG, Clare S, Matthews PM, Brady JM, Smith SM. Characterization and propagation of uncertainty in diffusion-weighted MR imaging. Magn ResonMed. 2003; 50(5):1077–1088.
14. Borghesani PR, Madhyastha TM, Aylward EH, Reiter MA, Swarny BR, Warner Schaie K, Willis SL. The association between higher order abilities, processing speed, and age are variably mediated by white matter integrity during typical aging. Neuropsychologia. 2013
15. Budde MD, Kim JH, Liang HF, Schmidt RE, Russell JH, Cross AH, Song SK. Toward accurate diagnosis of white matter pathology using diffusion tensor imaging. Magnetic resonance in medicine: official journal of the Society of Magnetic Resonance in Medicine/Society of Magnetic Resonance in Medicine. 2007; 57(4):688–695. [PubMed: 17390365]
16. Chen JY, Blankstein U, Diamant NE, Davis KD. White matter abnormalities in irritable bowel syndrome and relation to individual factors. Brain research. 2011; 1392:121–131. [PubMed: 21466788]

17. Costigan M, Scholz J, Woolf CJ. Neuropathic pain: a maladaptive response of the nervous system to damage. Annual review of neuroscience. 2009; 32:1–32.

18. Devor, M.; Seltzer, Z.; Wall, PD.; Melzack, R. Textbook of pain. Vol. 4. New York: Churchill-Livingstone; 1999. Pathophysiology of damaged nerves in relation to chronic pain; p. 129-164.

19. Geha PY, Baliki MN, Harden RN, Bauer WR, Parrish TB, Apkarian AV. The brain in chronic CRPS pain: abnormal gray-white matter interactions in emotional and autonomic regions. Neuron. 2008; 60(4):570–581. [PubMed: 19038215]

20. Gerdes JS, Keller SS, Schwindt W, Evers S, Mohammadi S, Deppe M. Progression of microstructural putamen alterations in a case of symptomatic recurrent seizures using diffusion tensor imaging. Seizure: the journal of the British Epilepsy Association. 2012; 21(6):478–481. [PubMed: 22546528]

21. Honey GD, Bullmore ET, Soni W, Varatheesan M, Williams SC, Sharma T. Differences in frontal cortical activation by a working memory task after substitution of risperidone for typical antipsychotic drugs in patients with schizophrenia. Proc Natl Acad Sci USA. 1999; 96(23):13432–13437. [PubMed: 10557338]

22. Johnson NF, Kim C, Gold BT. Socioeconomic status is positively correlated with frontal white matter integrity in aging. Age (Dordr). 2012

23. Lorenz J, Minoshima S, Casey KL. Keeping pain out of mind: the role of the dorsolateral prefrontal cortex in pain modulation. Brain: a journal of neurology. 2003; 126(Pt 5):1079–1091. [PubMed: 12690048]

24. Lutz J, Jager L, de Quervain D, Krauseneck T, Padberg F, Wichnalek M, Beyer A, Stahl R, Zirngibl B, Morhard D, Reiser M, Schelling G. White and gray matter abnormalities in the brain of patients with fibromyalgia: a diffusion-tensor and volumetric imaging study. Arthritis and rheumatism. 2008; 58(12):3960–3969. [PubMed: 19035484]

25. Matthews PM, Filippini N, Douaud G. Brain structural and functional connectivity and the progression of neuropathology in Alzheimer's disease. Journal of Alzheimer's disease: JAD. 2013; 33 (Suppl 1):S163–172.

26. McMillan CT, Brun C, Siddiqui S, Churgin M, Libon D, Yushkevich P, Zhang H, Boller A, Gee J, Grossman M. White matter imaging contributes to the multimodal diagnosis of frontotemporal lobar degeneration. Neurology. 2012; 78(22):1761–1768. [PubMed: 22592372]

27. Moayedi M, Weissman-Fogel I, Salomons TV, Crawley AP, Goldberg MB, Freeman BV, Tenenbaum HC, Davis KD. White matter brain and trigeminal nerve abnormalities in temporomandibular disorder. Pain. 2012; 153(7):1467–1477. [PubMed: 22647428]

28. Muller HP, Unrath A, Huppertz HJ, Ludolph AC, Kassubek J. Neuroanatomical patterns of cerebral white matter involvement in different motor neuron diseases as studied by diffusion tensor imaging analysis. Amyotrophic lateral sclerosis: official publication of the World Federation of Neurology Research Group on Motor Neuron Diseases. 2012; 13(3):254–264. [PubMed: 22409361]

29. O'Dwyer L, Lamberton F, Bokde AL, Ewers M, Faluyi YO, Tanner C, Mazoyer B, O'Neill D, Bartley M, Collins R, Coughlan T, Prvulovic D, Hampel H. Sexual dimorphism in healthy aging and mild cognitive impairment: a DTI study. PloS one. 2012; 7(7):e37021. [PubMed: 22768288]

30. Pfefferbaum A, Adalsteinsson E, Rohlfing T, Sullivan EV. Diffusion tensor imaging of deep gray matter brain structures: effects of age and iron concentration. Neurobiology of aging. 2010; 31(3): 482–493. [PubMed: 18513834]

31. Rodriguez-Raecke R, Niemeier A, Ihle K, Ruether W, May A. Brain gray matter decrease in chronic pain is the consequence and not the cause of pain. The Journal of neuroscience: the official journal of the Society for Neuroscience. 2009; 29(44):13746–13750. [PubMed: 19889986]

32. Seminowicz DA, Wideman TH, Naso L, Hatami-Khoroushahi Z, Fallatah S, Ware MA, Jarzem P, Bushnell MC, Shir Y, Ouellet JA, Stone LS. Effective treatment of chronic low back pain in humans reverses abnormal brain anatomy and function. The Journal of neuroscience: the official journal of the Society for Neuroscience. 2011; 31(20):7540–7550. [PubMed: 21593339]

33. Smith SM. Fast robust automated brain extraction. HumBrain Mapp. 2002; 17(3):143–155.

34. Smith SM, Jenkinson M, Johansen-Berg H, Rueckert D, Nichols TE, Mackay CE, Watkins KE, Ciccarelli O, Cader MZ, Matthews PM, Behrens TE. Tract-based spatial statistics: voxelwise

analysis of multi-subject diffusion data. NeuroImage. 2006; 31(4):1487–1505. [PubMed: 16624579]

35. Song SK, Sun SW, Ramsbottom MJ, Chang C, Russell J, Cross AH. Dysmyelination revealed through MRI as increased radial (but unchanged axial) diffusion of water. NeuroImage. 2002; 17(3):1429–1436. [PubMed: 12414282]
36. Stein N, Sprenger C, Scholz J, Wiech K, Bingel U. White matter integrity of the descending pain modulatory system is associated with interindividual differences in placebo analgesia. Pain. 2012; 153(11):2210–2217. [PubMed: 22959599]
37. Sullivan EV, Pfefferbaum A. Diffusion tensor imaging and aging. Neuroscience and biobehavioral reviews. 2006; 30(6):749–761. [PubMed: 16887187]
38. Teepker M, Menzler K, Belke M, Heverhagen JT, Voelker M, Mylius V, Oertel WH, Rosenow F, Knake S. Diffusion tensor imaging in episodic cluster headache. Headache. 2012; 52(2):274–282. [PubMed: 22082475]
39. Wang PN, Chou KH, Lirng JF, Lin KN, Chen WT, Lin CP. Multiple diffusivities define white matter degeneration in amnestic mild cognitive impairment and Alzheimer's disease. Journal of Alzheimer's disease: JAD. 2012; 30(2):423–437.

Summary

white matter fractional anisotropy (FA) differences accurately predicted back pain persistence over one year, and showed minimal alterations over the one year period.

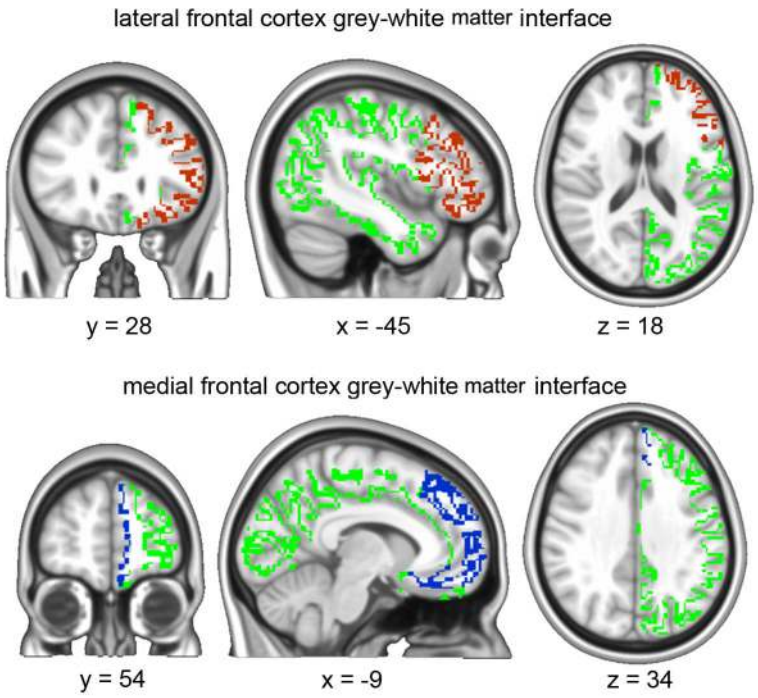

Figure 1.

Gray-to-White matter interface was identified for each subject (green). A standard brain atlas was then used to identify the lateral frontal cortex (red) and medial frontal cortex (blue). These masks were projected to individual space as targets for identifying structural connectivity.

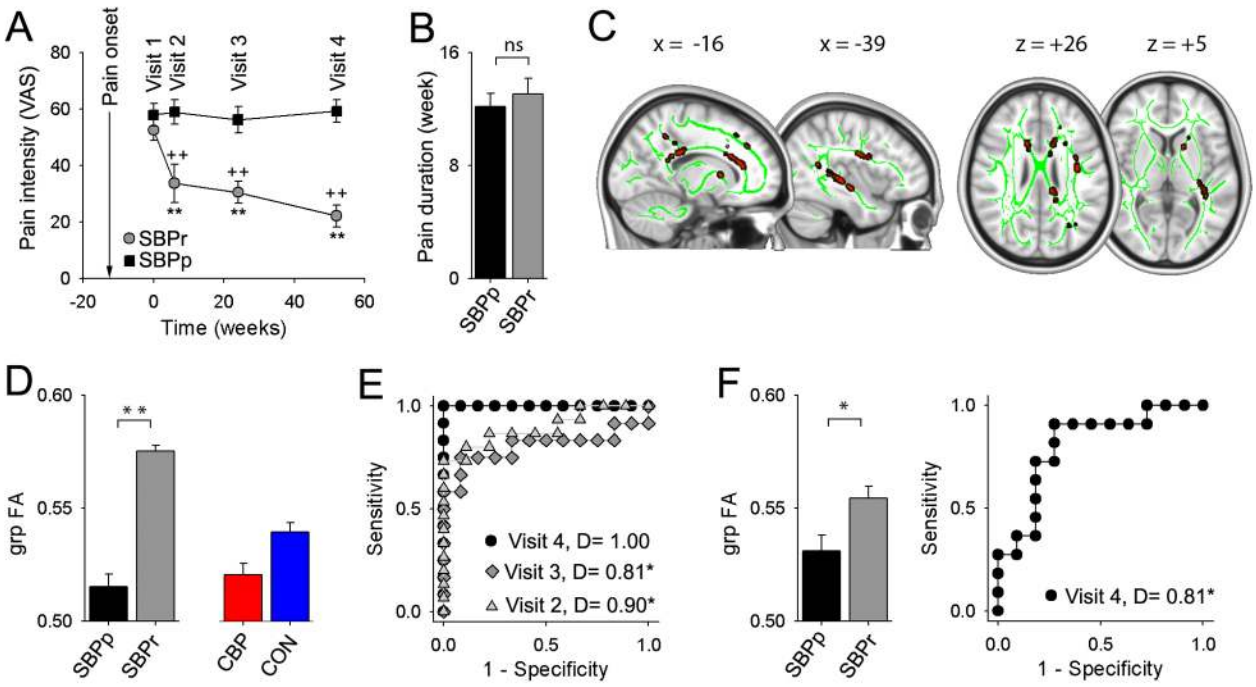

Figure 2. Regional FA differences at baseline distinguish SBPp from SBPr, and predict SBP groups one year later

(A) SBPr subjects (in contrast to SBPp) exhibited expected decreases in pain intensity with time (2-way repeat-measure ANOVA, group x time, $F_{3,114} = 10.27$, $p<0.001$) (SBPp, black; SBPr, gray). **(B)** Duration of back pain was similar between SBPr and SBPp ($t_{44} = -0.60$, $p = 0.55$). **(C)** Whole-brain white matter FA contrast (SBPr>SBPp), at visit 1 (baseline), and tested only in the Discovery-SBP group, identifies tracts (red; green = white matter skeleton) exhibiting significantly lower FA in SBPp (n = 24, $p <0.05$ corrected for multiple comparisons, z-stat > 3). **(D)** grp-FA is the average FA across all white matter voxels identified to differ between SBP groups in **C**, also measured in CBP and CON. One-way ANOVA across the 4 groups was significant ($F_{3, 72} = 23.55$, $p<0.001$). **(E)** ROC curves and discrimination probabilities (*D*, area under ROC curve) for predicting pain persistence at visits 2, 3 and 4 based on Mean-FA at visit 1. (**F**) In a separate Validation-SBP group (n = =2.7, p=0.014), and 22), Mean-FA at visit 1 distinguishes SBPp and SBPr (t_{20} ROC and *D* values at visit 1 predicted persistence of pain at visit 4 (unbiased estimate). $^{+}P < 0.05$, $^{++}P < 0.01$, within group comparison to visit 1; $^{*}P < 0.05$, $^{**}P < 0.01$ across group comparison at corresponding times. Error bars represent S.E.M. SBPp=Sub-acute back pain - persistent; SBPr = Sub-acute back pain - recovering; CON = healthy controls; CBP = chronic back pain.

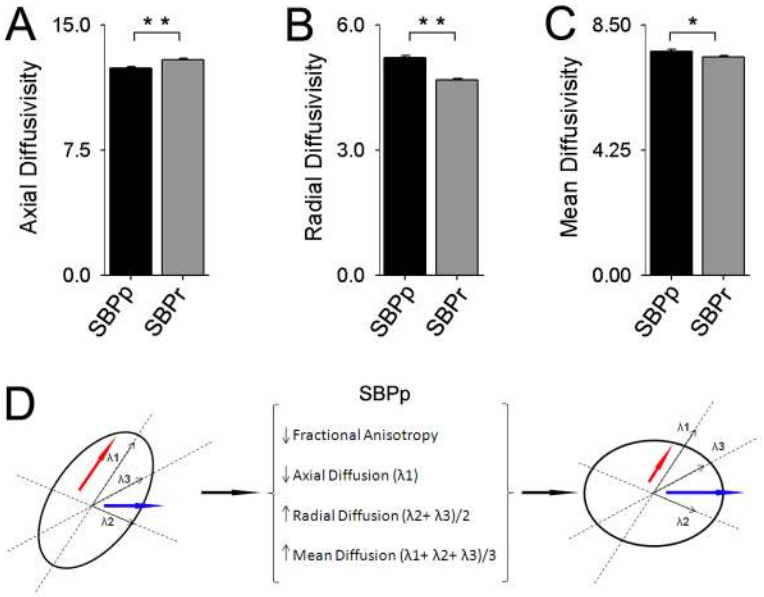

Figure 3. Diffusivity properties for white matter tracts where FA was lower in SBPp

Diffusivity differences were examined for the grp-FA mask at visit 1: **(A**) Axial diffusion was decreased in SBPp ($t_{22} = -4.68$, $p < 0.01$); **(B)** Radial diffusion increased in SBPp ($t_{22} = 7.39$, $p < 0.01$); and **(C)** Mean diffusion increased in SBPp ($t_{22} = 2.61$, $p = 0.016$), demonstrating that the increase in radial diffusion outweighs the decrease in axial diffusion. All three bargraphs are in units $10^{-4} \times mm^2$/second. **(D)** Schematic representing the relationship between fractional anisotropy and component diffusion parameters. Axial (red arrow) and Radial (blue arrow) Diffusions are shown in an ellipsoid representing the tensor for a given white matter voxel. For regions showing reduced FA, SBPp patients have reduced axial and increased radial diffusion (increasing MD), thus making the ellipsoid more spherical, resulting in reduced FA.

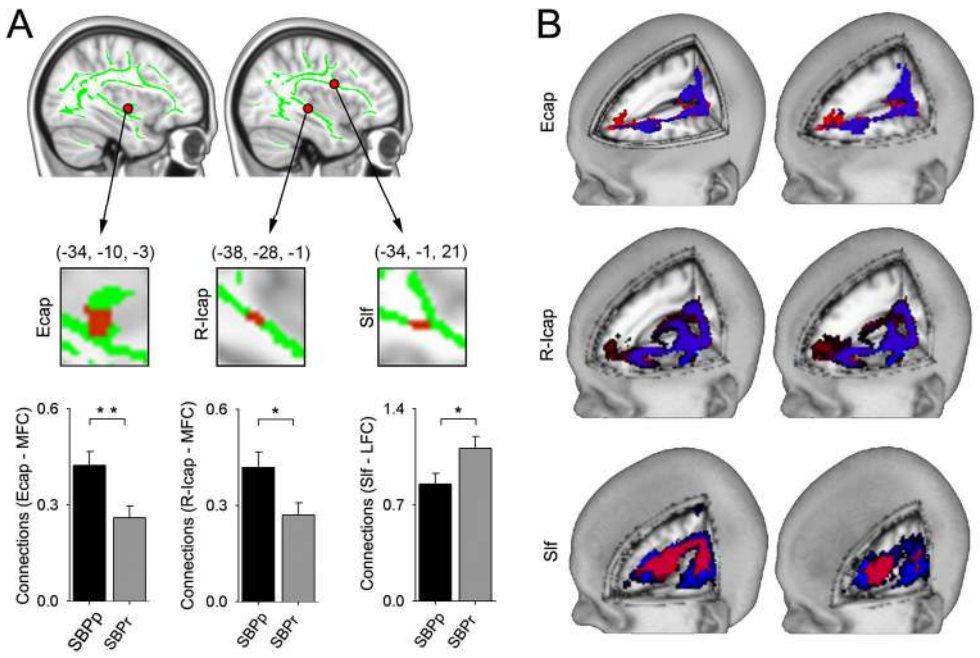

Figure 4. Differential structural connectivity to medial and lateral prefrontal cortex for tracts where FA was lower in SBPp

(A) White matter seeds (Ecap, R-Icap, Slf, red; green = white matter skeleton; derived from regions with decreased FA in SBPp in discovery-SBP at visit 1), that differentially connect with medial (MFC) and lateral (LFC) prefrontal cortex (tested for all SBP, n=46). In SBPp, Ecap (t_{44} = 2.87, p = 0.006) and r-Icap (t_{44} = 2.38, p = 0.022) show higher connectivity to the medial prefrontal cortex; while in SBPr, slf shows higher connectivity to lateral prefrontal cortex (t_{44} = −2.223, p = 0.031). (B) Tractography schematic showing group mean tracts seeded from Ecap and r-Icap more connected to MFC in SBPp (red) whereas the group mean tracts seeded from slf are more connected to the LFC in SBPr (blue). *P < 0.05, **P < 0.01. Error bars represent S.E.M. slf= superior longitudinal fasciculus; Ecap =external capsule; r-Icap= retro-lenticular limb of internal capsule.

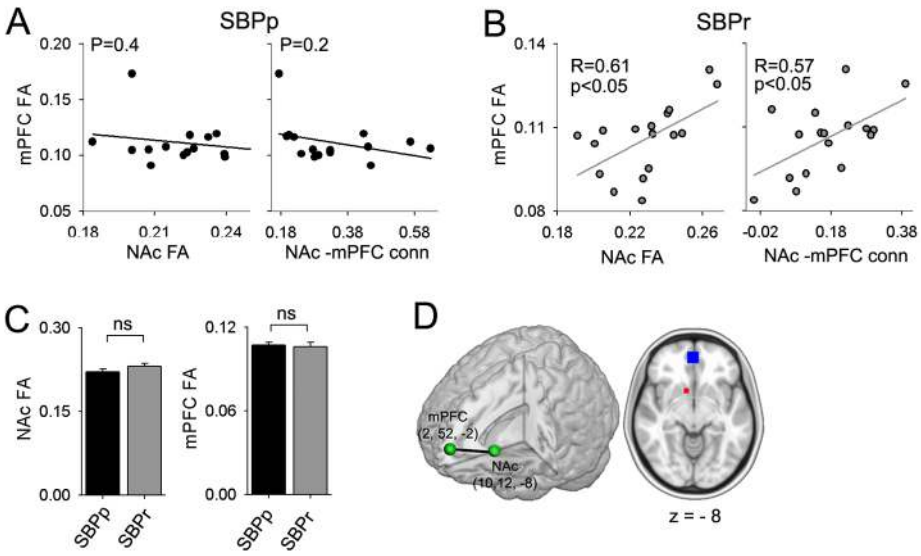

Figure 5. mPFC-NAc functional connectivity is differentially related to FA in mPFC

(A) In SBPp, NAc FA does not correlate to mPFC FA; and NAc-mPFC functional connectivity does not correlate with FA in mPFC. **(B)** In SBPr, NAc FA positively correlated with mPFC FA; and NAc-mPFC functional connectivity also positively correlated with FA in mPFC. **(C)** Neither NAc FA nor mPFC FA were different across the two groups (t_{29}=0.22, p=0.83 and t_{29}=−1.41, p=0.17 for mPFC and NAc respectively). **(D)** Coordinates and size of regions from which mPFC-NAc functional connectivity and mean FA for NAc (red) and mPFC (blue) were calculated. These values are derived from our earlier study [9]. Error bars represent S.E.M. ns = not significant.

Table 1

Clinical pain and mood parameters

Data shows the pain and mood characteristics at visit 1 (12 weeks after back pain onset), visit 4 (one year after back pain onset) and across time, for recovering and persisting back pain (SBPr and SBPp). None of the questionnaire outcomes showed a significant difference between SBP groups at visit 1. Pain related outcomes decreased in SBPr at visit 4, relative to visit 1 and relative to SBPp.

	VISIT 1			VISIT 4			VISIT 4 > VISIT 1	
	SBPp	**SBPr**	**SBPp>SBPr t-values**	**SBPp**	**SBPp**	**SBPp>SBPr t-values**	**SBPp**	**SBPr**
VAS (0–100)	57.9 ± 3.9	52.6±3.8	+0.99 (ns)	59.3 ± 3.9	22.2 ± 3.9	+6.65 **	ns	**
Duration (weeks)	12.2 ± 1.0	13.1 ± 1.1	−0.6 (ns)	65.7 ± 1.0	68.0 ± 1.3	−1.4 (ns)	--	--
MPQ sensory	12.9 ± 1.4	9.8 ± 0.9	+1.8 (ns)	12.46 ± 1.4	7.1 ± 1.4	+2.8 **	ns	*
MPQ affective	3.3 ± 0.6	1.8 ± 0.4	+1.9 (ns)	3.1 ± 0.7	1.4 ± 0.5	+2.1**	ns	ns
MPQ radiculopathy	5.6 ± 0.5	4.5 ± 0.3	+1.4 (ns)	5.7 ± 0.5	3.3 ± 0.5	+4.1**	ns	**
NPS	45.1 ± 4.1	35.5 ± 3.1	+1.8 (ns)	40.7 ± 3.9	18.3 ± 2.8	+4.8**	ns	**
BDI	7.8 ± 1.0	7.5 ± 1.2	+0.09 (ns)	5.6 ± 1.4	4.3 ± 1.2	+0.7 (ns)	ns	ns
PANAS positive	33.6 ± 1.7	30.9 ± 11.0	+1.01 (ns)	32.5 ± 1.8	33.3 ± 1.5	- 0.3 (ns)	ns	ns
PANAS negative	19.4 ± 1.6	17.7 ± 1.9	+0.90 (ns)	19.4 ± 1.4	15.7 ± 1.3	+1.9 (ns)	ns	ns

VAS=visual analogue scale; MPQ = McGill pain questionnaire; NPS = Neuropathic pain scale; BDI = Beck's depression index. PANAS = Positive Affect Negative Affect Scale.

Values are Mean ±SEM;(-- = not applicable; ns = not significant. * p<0.05, ** p<0.01).

Table 2

Structural connectivity changes

Data shows the changes in structural connectivity between white matter seeds and medial or lateral frontal cortex, over one year (visit 1 to visit 4), in persisting and recovering back pain (SBPp and SBPr). Values are normalized probability of structural connectivity between white matter seeds and medial and lateral prefrontal cortices. Ecap, r-Icap, slf are white matter seeds, shown in figure 3A.

	SBPp			SBPr		
	Visit 1	**Visit 4**	**Visit 4>Visit 1 t-values**	**Visit 1**	**Visit 4**	**Visit 4>Visit 1 t-values**
Ecap - mfc	0.395 ±0.060	0.260 ± 0.057	- 2.06 (ns)	0.296 ±0.060	0.301 ±0.057	+ 0.09 (ns)
R-Icap - mfc	0.392 ± 0.076	0.234 ± 0.042	- 1.844 (ns)	0.318 ±0.063	0.471 ±0.0778	+ 2.21 (ns)
slf - lfc	0.858 ± 0.096	0.943 ± 0.164	+ 0.556 (ns)	1.134 ± 0.110	1.869 ± 0.107	+ 6.030**

mfc = the grey-white matter edge of the whole medial prefrontal cortex; lfc = the grey-white matter edge of the whole lateral prefrontal cortex, see figure 1.

Values are Mean ±SEM. (ns = not significant; ** $p < 0.01$)